NACA

RESEARCH MEMORANDUM

FLIGHT TESTS AT TRANSONIC AND SUPERSONIC SPEEDS OF AN AIRPLANE-LIKE CONFIGURATION WITH THIN STRAIGHT SHARP-EDGE WINGS AND TAIL SURFACES

By

Clarence L. Gillis and Jesse L. Mitchell

Langley Aeronautical Laboratory
Langley Field, Va.

NATIONAL ADVISORY COMMITTEE
FOR AERONAUTICS

WASHINGTON

January 5, 1949

Classification cancelled (or changed to) Unclassified

By authority of: Nasa Tech Pub Announcement #22
(OFFICER AUTHORIZED TO CHANGE)

By ..... 3 Dec 57

NK

(GRADE OF OFFICER MAKING CHANGE)

20 Nov 61
DATE

NATIONAL ADVISORY COMMITTEE FOR AERONAUTICS

RESEARCH MEMORANDUM

FLIGHT TESTS AT TRANSONIC AND SUPERSONIC SPEEDS OF AN AIRPLANE-LIKE CONFIGURATION WITH THIN STRAIGHT SHARP-EDGE WINGS AND TAIL SURFACES

By Clarence L. Gillis and Jesse L. Mitchell

SUMMARY

Rocket-powered models of a representative airplane configuration were flight-tested at the Langley Pilotless Aircraft Research Division testing station at Wallops Island, Va. The configuration tested had a slender pointed-nose fuselage and unswept low-aspect-ratio wing and tail surfaces with thin faired double-wedge airfoil sections. The Mach number range covered in the tests was from 0.5 to 1.4.

The results showed a positive change in trim normal-force coefficient of about 0.4 (with the center of gravity at 16 percent of the mean aerodynamic chord) between Mach numbers of 0.8 and 1.0 for a constant horizontal tail setting. This change would amount to about 2.7g normal acceleration for an airplane with a wing loading of 100 pounds per square foot and at an altitude of 20,000 feet. The effectiveness of the horizontal tail in changing the trim normal-force coefficient is about 60 percent smaller at supersonic speeds than at subsonic speeds. A change in tail deflection of about 5° in a trailing-edge-down direction is required for level flight as the Mach number increases from 0.6 to 1.0 and a change of 3° in the trailing-edge-up direction is required as the Mach number increases from 1.0 to 1.4.

At a Mach number of 0.5 the trim lift-curve slope is about 0.08 and the neutral point is at about 40 percent of the mean aerodynamic chord. No such quantitative data were obtained at supersonic speeds, but the data indicate that with the center of gravity at 16 percent of the mean aerodynamic chord the model has positive longitudinal stability throughout the speed range covered by the tests.

The directional stability of the model appears to be adequate throughout the speed range tested with a value of the directional stability parameter C_{n_β} of 0.005 at a Mach number of 0.5, and 0.016 at a Mach number of 1.15.

The trim change and drag break both begin at a Mach number of 0.85 which agrees with wind-tunnel drag measurements for a wing similar to that used on the rocket models.

INTRODUCTION

Many configurations of airplanes and airplane components have been proposed for attaining good flight characteristics throughout a speed range which includes the supersonic. Some data exist on the drag and control effectiveness at zero lift of some of these components (references 1 and 2, for example). There are few data on the lift and stability characteristics at transonic and low supersonic speeds of airplane configurations using these components. As a part of a program to obtain such data, rocket-powered models of a configuration representing a possible supersonic airplane were flight-tested. The model had a slender pointed-nose fuselage and unswept low-aspect-ratio wing and tail surfaces having thin faired double-wedge airfoil sections. The models were flown with various fixed horizontal-tail settings and center-of-gravity positions to obtain information on the trim, stability, and control-effectiveness characteristics at transonic and low supersonic speeds. This series of models was the first for which the test technique described has been used. Five models were flown at the Langley Pilotless Aircraft Research Division testing station at Wallops Island, Va.

SYMBOLS

C_N	normal-force coefficient $\left(\frac{a_n}{g}\frac{W/S}{q}\right)$
C_c	chord-force coefficient $\left(\frac{a_l}{g}\frac{W/S}{q}\right)$
C_n	yawing-moment coefficient
a_n	normal acceleration, feet per second per second
a_l	longitudinal acceleration, feet per second per second
a_t	transverse acceleration, feet per second per second
g	acceleration of gravity, feet per second per second
M	Mach number
H	total-head pressure, pounds per square foot
p	free-stream static pressure, pounds per square foot
q	dynamic pressure, pounds per square foot $\left(\frac{\gamma}{2}pM^2\right)$

γ	specific heat ratio (1.40)
W	weight
S	wing area, square feet
$\bar{c}$	wing mean aerodynamic chord, feet
α	angle of attack, measured from fuselage reference line, degrees
β	sideslip angle, degrees
δ	deflection of horizontal tail, measured from fuselage reference line; positive in trailing-edge-down direction
$\frac{pb}{2V}$	wing-tip helix angle, radians
t	time from launching, seconds
C_{n_β}	directional stability derivative $(dC_n/d\beta)$
C_{m_α}	longitudinal stability derivative $\left(dC_m/d_\alpha\right)$
I_y	moment of inertia about y-axis, slug-feet^2
I_z	moment of inertia about z-axis, slug-feet^2
C_D	drag coefficient $(C_C \cos \alpha + C_N \sin \alpha)$

Abbreviation:

TE	trailing edge

MODELS AND APPARATUS

A three-view drawing of the model is shown in figure 1. The airframes were of dural and magnesium construction. The wings and tail surfaces were made of solid dural and the fuselage was of semimonocoque construction with a stressed skin of magnesium. Photographs of a model with an angle-of-attack indicator installed on the nose are shown in figure 2.

Models 2, 3, and 4 were flown with a vertical tail having an area 25 percent greater than that shown in figure 1. A sketch of the enlarged vertical tail is shown in figure 3. The vertical tail and ailerons were

set at zero deflection for all flights. The wing was set at zero incidence with respect to the fuselage reference line. The longitudinal control consisted of an adjustable stabilizer, the setting of which was adjusted prior to flight by means of a surface plate and height gage. For models 2 to 5 the wing-fuselage and tail-fuselage junctures were faired with doped aircraft fabric.

The motive power consisted of a 5-inch HVAR booster with a similar sustaining rocket in the model. Both rockets were modified to give a thrust of about 3500 pounds for a period of 1.5 seconds and the sustaining rocket was fitted with a high-pressure blast tube (fig. 1) to permit location of the rocket farther forward in the model. Separation of the booster from the model was accomplished either by the drag of the booster or by the firing of the sustaining rocket.

The models were launched from a zero-length launcher at an elevation angle of approximately 45°. Photographs of a model on the launcher are shown in figure 4.

Models 1 to 4 were equipped with telemeters transmitting continuous measurements of normal, longitudinal, and transverse accelerations, in addition to total-head pressure as measured by an orifice at the nose of the model. Model 5 contained a telemeter measuring the above quantities plus angle of attack. In addition to the instrumentation in the models, a CW Doppler radar unit was available for measuring model velocity, and a tracking radar was available for obtaining range and elevation as a function of time. Atmospheric conditions were determined from a radiosonde released at the time of firing.

Fixed wide-angle cameras and 16-millimeter motion-picture cameras recorded the launching. The flights were tracked for the first 4 to 5 seconds by 16-millimeter motion-picture cameras. Pictures of a typical launching taken with the wide-angle camera are shown in figure 5.

TESTS

The testing technique used was that of measuring the variation, with Mach number, of trim normal-force coefficients at a constant horizontal-tail deflection. From two or more models having different tail deflections, but the same center-of-gravity location, these data will give a measure of control effectiveness, $\frac{\Delta C_N}{\Delta \delta}$. A plot of the inverse function, $\frac{\Delta \delta}{\Delta C_N}$, against center-of-gravity location can be extrapolated to zero to obtain maneuver points. The horizontal-tail deflections and center-of-gravity locations used in these tests, along with the weights and moments of inertia of the models, are given in table I. The moments of inertia were determined by swinging the model as a pendulum and timing the oscillations.

[redacted]

The Mach number was computed from the following relations:

(a) subsonic

$$\frac{H}{p} = \left(1 + \frac{\gamma - 1}{2} M^2\right)^{\frac{\gamma}{\gamma-1}}$$

(b) supersonic

$$\frac{H}{p} = \frac{\left(\frac{\gamma + 1}{2} M^2\right)^{\frac{\gamma}{\gamma-1}}}{\left(\frac{2\gamma}{\gamma + 1} M^2 - \frac{\gamma - 1}{\gamma + 1}\right)^{\frac{1}{\gamma-1}}}$$

where H was measured by the total-head tube on the nose of the model, and p was obtained from altitude and radiosonde data.

The Mach numbers given in figures 6 to 10 are subject to some inaccuracies. The methods available at present for determining the Mach numbers for maneuvering models do not give values as accurately as is desired for models exhibiting large gradients of trim lift coefficient with Mach number as occurred on this configuration. Model 3 should have the most nearly correct values of Mach number. For models 1, 3, and 4 the Mach numbers shown are believed to be correct within ±0.02 near $M = 1.0$ with somewhat better accuracy at higher Mach numbers and somewhat worse at lower Mach numbers. For model 2, there appears to be a possible error of +0.05 in Mach number near $M = 1.0$.

The Reynolds number based on the wing mean aerodynamic chord varied from 5×10^6 at a Mach number of 0.6 to 11×10^6 at a Mach number of 1.4 for all flights.

A chronological review of the test flights will serve to show the reasons for the modifications made on the models during the test program and to clarify the subsequent discussion of test results.

Model 1.- After booster separation the model began a slow roll to the left and followed a helical path. An examination of the motion pictures of this flight indicated that the rate of roll amounted to a value of $pb/2V$ of about 0.0035. Preliminary reduction of the telemetered data showed very small normal acceleration throughout the speed range but indicated large transverse accelerations in the transonic and supersonic range. It was therefore concluded that the model had unsatisfactory directional characteristics and a larger vertical tail was designed for subsequent flights, as mentioned previously.

Model 2.- This model also began a slow roll to the left after booster separation but appeared to be rolling more slowly than model 1. The telemeter record showed large changes in normal acceleration through the speed range with practically zero transverse acceleration throughout.

Model 3.- This model was intended to be trimmed for practically zero lift as was model 1 but had a different center-of-gravity location from model 1. It was therefore expected to have normal acceleration values very similar to that of model 1. After booster separation the model pulled up into an almost vertical path and did not appear to have any roll during the time it was visible. A cursory examination of the telemeter record indicated large changes in normal acceleration through the speed range. Comparing this flight with those of models 1 and 2 it was concluded that the results for model 1 were in error, apparently caused by inadvertent interchange of the normal and transverse accelerometers after the preflight instrument calibration had been completed.

Model 4.- This model had been prepared for flight at the same time as model 3 and had the large vertical tail. Although it was now believed that the larger vertical tail was unnecessary for directional stability, the effect of vertical-tail size on the longitudinal characteristics was believed to be negligible and did not warrant delaying the test to remove the larger tail. Model 4 also rolled to the left after booster separation at a rate which appeared to be slower than that of model 1.

Model 5.- As a result of previous flights, it was concluded that the large vertical tail was unnecessary so this model was flown with the original tail. It was considered desirable to incorporate an instrument for measuring angle of attack so that the data could be computed as lift and drag coefficients as well as normal- and chord-force coefficients. The flight of this model was only partially successful as the sustainer failed to fire; however, the booster separated from the model at burnout due to drag and some data were obtained at subsonic speeds.

RESULTS AND DISCUSSION

Time-History Records

Time histories of the important parts of flight for models 1 to 5 are given in figures 6 through 10. The most interesting feature of the flights is the large change in normal acceleration as the model traverses the transonic speed range. The change in trim on model 3, for example, was from 0.1g at $M = 0.8$ to 18.4g at $M = 1.1$. This trim change of 18.3g would amount to 2.7g on a similar configuration with a wing loading of 100 pounds per square foot and at an altitude of 20,000 feet. The change is observed both in the power-on and the power-off parts of the flight. The magnitudes of the normal accelerations are not the same for power-on and power-off flight at the same Mach

number because of power effects. At supersonic speeds these effects can be accounted for largely by thrust misalinement and varying weight during powered flight. At subsonic speeds these same effects are present but are augmented by the effect of the inflow into the jet causing a downflow over the horizontal tail. This latter effect is discussed in references 3 and 4. The inflow effect would be considerably less on a full-scale airplane because of the smaller thrust coefficients used.

As explained previously, the normal and transverse accelerometers on model 1 apparently were interchanged after calibration and it was possible to get only approximate values of normal and transverse accelerations on this flight. The approximate normal and transverse accelerations are shown as dotted lines on the time history (fig. 6). A zero shift in the longitudinal acceleration channel occurred on model 2 at take-off, as evidenced on the telemeter record by the much more positive values of acceleration than occurred on the other models. The curve was therefore shifted along the acceleration axis to give more reasonable values. The resulting curve is shown dotted in figure 7, but the data have not been used in the subsequent analysis. The variation of the factor $\frac{W/S}{q}$ with time for all models is presented in figure 11. The effect on the longitudinal characteristics of the rolling velocity that was obtained on most of the models was investigated analytically by the method of reference 5 and found to be negligible.

Longitudinal Trim and Control Effectiveness

In figure 12 the normal-acceleration data from the time histories have been reduced to normal-force coefficients and plotted against Mach number. In figure 12(a) the variation with Mach number of trim normal-force coefficient for model 2 is shown as a dotted line and is presented for qualitative analysis only. At the rearward center-of-gravity position (fig. 12(b)) a change of about 0.4 in trim normal-force coefficient occurs in traversing the transonic region. It is to be noted that this trim change begins at approximately $M = 0.85$, the Mach number at which the drag rise also begins. (See figs. 13 and 14.) Wind-tunnel tests on a wing similar to that on these models (reference 6) indicate that the Mach number for drag divergence of the wing alone is also 0.85.

Figure 15 has been derived from figure 12 and shows the variation of control effectiveness $\frac{\Delta C_N}{\Delta \delta}$ with Mach number at the average rearward center-of-gravity position $(0.16\bar{c})$.

Because of incomplete data between $M = 0.6$ and $M = 0.85$ and because of the steep gradient of C_N against M near $M = 0.9$ (see fig. 12(b)), the portion of the curve below 0.95 is doubtful and is shown dotted. A decrease of about 60 percent in control effectiveness between

subsonic and supersonic speeds is indicated, with an even larger drop near $M = 1.0$. The values of $\frac{\Delta C_N}{\Delta \delta}$ in figure 15 are subject to some uncertainty because of small increments between the curves of figure 12(b).

Some values of $\frac{\Delta C_N}{\Delta \delta}$ were estimated from unpublished wind-tunnel data on a similar airplane configuration and these are shown in figure 15 for comparison with the measured values. The measured $\frac{\Delta C_N}{\Delta \delta}$ is somewhat lower than that indicated by the wind-tunnel data throughout the Mach number range tested.

Included in figure 12(b) is a curve of normal-force coefficient required for trim in level flight for the airplane configuration with a wing loading of 100 pounds per square foot and at an altitude of 20,000 feet. The values plotted are actually lift coefficients but, for the small angles of attack involved, lift coefficient and normal-force coefficient can be considered equal. The horizontal-tail deflection for trim under these conditions is shown in figure 16. Although most of the values in figure 16 represent linear extrapolations of the measured data (see fig. 12(b)), it is believed that the curve gives a fairly good indication of the trim changes that can be expected with this configuration. A total change in horizontal-tail deflection for trim of about 5° in the trailing-edge-down direction is necessary in accelerating from $M = 0.6$ to $M = 1.0$ with a further change of about 3° in the trailing-edge-up direction from $M = 1.0$ to $M = 1.4$.

Results of tests on a similar airplane configuration by the wing-flow method (reference 7) indicated changes of longitudinal trim and control effectiveness with Mach number that are not as large or as abrupt as the variations obtained on the rocket-powered models. The reasons for the differences are not definitely known but are probably explained by the following differences in testing technique: The Reynolds numbers for the rocket models were of the order of 5×10^6 to 10×10^6 while those for the wing-flow model were about 0.5×10^6; the air flow over the wing-flow model had a Mach number gradient both spanwise and chordwise (reference 7), and because of the method of construction and the lower test dynamic pressures the wing-flow model was less flexible than the rocket models. The wing torsional stiffness of the rocket models may be found by applying a scale factor to the data of figure 3, reference 8, which gives measured values of the torsional stiffness for geometrically similar wings constructed of the same material. It may also be pointed out that wing-fuselage interference effects, which may be large on this type model, (reference 9) are difficult to simulate on a wing-flow model.

As stated in the description of the testing technique, the data desired from the tests were records of trim normal-force coefficient as a function of Mach number. Since the model is decelerating constantly during the time the data are taken and the abrupt changes in normal

force take place during a small time interval (about 1 to 2 sec), there was some doubt that the model would actually be trimmed. This effect was investigated prior to the tests by making a stepwise calculation of the model motion from $M = 1.05$ to $M = 0.90$ on the Bell Telephone Laboratories X-66744 relay computer at the Langley Laboratory using time intervals of 0.001 second. The aerodynamic data used were from wind-tunnel tests on a transonic "bump" of a somewhat different airplane configuration exhibiting trim changes in the transonic region of the same order of magnitude as those occurring on the models described herein. The results of the calculations showed that the model would at all times be within 0.1° of the trim angle of attack which is well within the experimental accuracy.

Longitudinal Stability

Due to the doubtful accuracy of the normal-acceleration data on model 1 it is believed that maneuver points determined from those data cannot be considered reliable and are thus not presented. However, the data indicate positive stability throughout the speed range.

It is possible to obtain an approximate value of the longitudinal stability by applying the method of reference 10 to the oscillations in normal acceleration. This method is less exact when applied to pitch oscillations, however, than when applied to yaw oscillations because of the assumptions used in deriving the method. Model 5 was the only one for which a well-defined and fairly regular oscillation in pitch occurred. An average value of $C_{m_\alpha} = -0.020$ at a Mach number of 0.5 is obtained from this oscillation, which indicates a neutral point location at about $0.40\bar{c}$ for a lift-curve slope of 0.08 (see discussion of lift and drag). An attempt was made to calculate the stability from random oscillations occurring during the flights of models 1 to 4. The results gave values which had a very wide scatter and it is believed that these rather small and irregular oscillations do not give a reliable indication of the stability of the model.

Directional Stability

All of the models flown showed an oscillation of the transverse acceleration. For models 1 to 4 this oscillation occurred only above $M = 0.85$. From the periods of these oscillations and the method of reference 10 values of C_{n_β}, the directional stability derivative, were calculated. The moment of inertia in yaw I_Z required for these calculations was not measured on the models. It was assumed that for this type of model I_Z would be nearly equal to I_Y, which was used in the calculation of C_{n_β}. The values of C_{n_β} are shown in figure 17 and are for the two different center-of-gravity positions and the two tail sizes since the effects of these variables on the values of C_{n_β}

[redacted]

are within the experimental accuracy. This method of computing stability parameters also neglects damping and the product of inertia term (reference 11) both of which have a small effect on the period of oscillation. The data show adequate directional stability throughout the Mach number range covered, C_{n_β} for the original model varying from 0.005 at $M = 0.5$, to 0.016 at $M = 1.15$. Unpublished wind-tunnel tests on a similar airplane configuration indicate good agreement with the values of C_{n_β} in figure 17.

Chord-Force Coefficients

Figure 13 shows the variation of power-off chord-force coefficient with Mach number. The sharp increase through the transonic range is characteristic and as expected. No data are presented for model 2 due to the indeterminate zero shift of the longitudinal acceleration channel.

Lift and Drag

As explained previously, model 5 was equipped with an angle-of-attack indicator so that the normal-force and chord-force data could be reduced to lift and drag coefficients. No lift and drag data are presented for this model, however, as the recorded values of angle of attack indicate a zero shift in the instrument of about $+1\frac{1}{2}^\circ$ to $+2^\circ$. This error may be due to some asymmetry in the angle-of-attack vane which causes it to float at some angle of attack other than zero, or a zero shift in the telemeter frequency. The angle-of-attack data presented in figure 10 have not been corrected for this zero shift nor have they been corrected for the effect of flight-path curvature and rate of change of angle of attack with respect to time. The variations with angle of attack of the normal-force coefficients are believed to be correct however. Using these data, $\frac{\Delta C_N}{\Delta \delta}$ averages 0.08 for a Mach number of approximately 0.5 which is a reasonable value for this configuration.

An evaluation of the trim-drag coefficients can be made using the normal-force and chord-force data of this report and the angle-of-attack data of reference 7. The results for models 3 and 4 are given in figure 14.

CONCLUSIONS

From the results of flight tests of rocket-powered models of a representative airplane configuration through the transonic region, the following conclusions are indicated:

1. At a constant horizontal-tail setting and center of gravity at 16 percent of the mean aerodynamic chord there is a change of about 0.4 in trim normal-force coefficient between Mach numbers of 0.8 and 1.0. This change is in a positive direction with increasing Mach number and would amount to 2.7g normal acceleration on a similar airplane with a wing loading of 100 pounds per square foot and flying at 20,000 feet.

2. The effectiveness of the horizontal tail in changing the trim normal-force coefficient of the airplane is roughly 60 percent smaller at supersonic speeds than at subsonic speeds with an indication of an even larger drop at a Mach number of 1.0.

3. A change in horizontal-tail deflection of about 5° in the trailing-edge-down direction is required for level flight as the Mach number increases from 0.6 to 1.0 with a further change of 3° in the trailing-edge-up direction as the Mach number increases from 1.0 to 1.4.

4. The directional stability of the model appears to be adequate throughout the speed range tested with values of the directional-stability parameter C_{n_β} varying from 0.005 at $M = 0.5$ to 0.016 at $M = 1.15$. Fairly regular directional oscillations of small amplitude occurred on all the models.

5. At a Mach number of 0.5 the trim lift-curve slope is about 0.08 and the neutral-point location is at about 40 percent of the mean aerodynamic chord. No such data were obtained at supersonic speeds.

6. The trim change and drag break both begin at a Mach number of 0.85 which agrees with wind-tunnel drag measurements on a wing similar to that used on the rocket models.

Langley Aeronautical Laboratory
National Advisory Committee for Aeronautics
Langley Field, Va.

REFERENCES

1. Tucker, Warren A., and Nelson, Robert L.: Drag Characteristics of Rectangular and Swept-Back NACA 65-009 Airfoils Having Various Aspect Ratios as Determined by Flight Tests at Supersonic Speeds. NACA RM No. L7C05, 1947.

2. Sandahl, Carl A.: Free-Flight Investigation of Control Effectiveness of Full-Span, 0.2-Chord Plain Ailerons at High Subsonic, Transonic, and Supersonic Speeds to Determine Some Effects of Wing Sweepback, Taper, Aspect Ratio, and Section Thickness Ratio. NACA RM No. L7F30, 1947.

3. Squire, H. B., and Trouncer, J.: Round Jets in a General Stream. R. & M. No. 1974, British A.R.C., 1944.

4. Ribner, Herbert S.: Field of Flow about a Jet and Effect of Jets on Stability of Jet-Propelled Airplanes. NACA ACR No. L6C13, 1946.

5. Phillips, William H.: Effect of Steady Rolling on Longitudinal and Directional Stability. NACA TN No. 1627, 1948.

6. Johnson, Ben H., Jr.: Investigation of a Thin Wing of Aspect Ratio 4 in the Ames 12-Foot Pressure Wind Tunnel. I - Characteristics of a Plain Wing. NACA RM No. A8D07, 1948.

7. Silsby, Norman S., and McKay, James M.: Longitudinal Stability and Control Characteristics of a Semispan Model of a Supersonic Airplane Configuration at Transonic Speeds from Tests by the NACA Wing-Flow Method. NACA RM No. L8G30, 1948.

8. Sandahl, Carl A.: Free-Flight Investigation at Transonic and Supersonic Speeds of the Rolling Effectiveness of a Thin, Unswept Wing Having Partial-Span Ailerons. NACA RM No. L8G20a, 1948.

9. Van Dyke, Milton D.: Aerodynamic Characteristics Including Scale Effect of Several Wings and Bodies Alone and in Combination at a Mach Number of 1.53. NACA RM No. A6K22, 1946.

10. Bishop, Robert C., and Lomax, Harvard: A Simplified Method for Determining from Flight Data the Rate of Change of Yawing-Moment Coefficient with Sideslip. NACA TN No. 1076, 1946.

11. Sternfield, Leonard: Effect of Product of Inertia on Lateral Stability. NACA TN No. 1193, 1947.

TABLE I

[The following data apply to the unpowered portion of the flights.]

Model	Weight (lb)	Center-of-gravity position (percent M.A.C.)	[1]Moment of inertia, I_y (slug-ft^2)	Horizontal tail setting (deg)
1	128.6	-4.2	30.4	0
2	134.3	-4.7	34.4	-1.72
3	128.8	16.4	30.7	0.12
4	127.8	16.6	30.3	1.00
5	149.9	15.7	27.2	2.4

[1]For calculating C_{n_β} it was assumed that $I_z = I_y$.

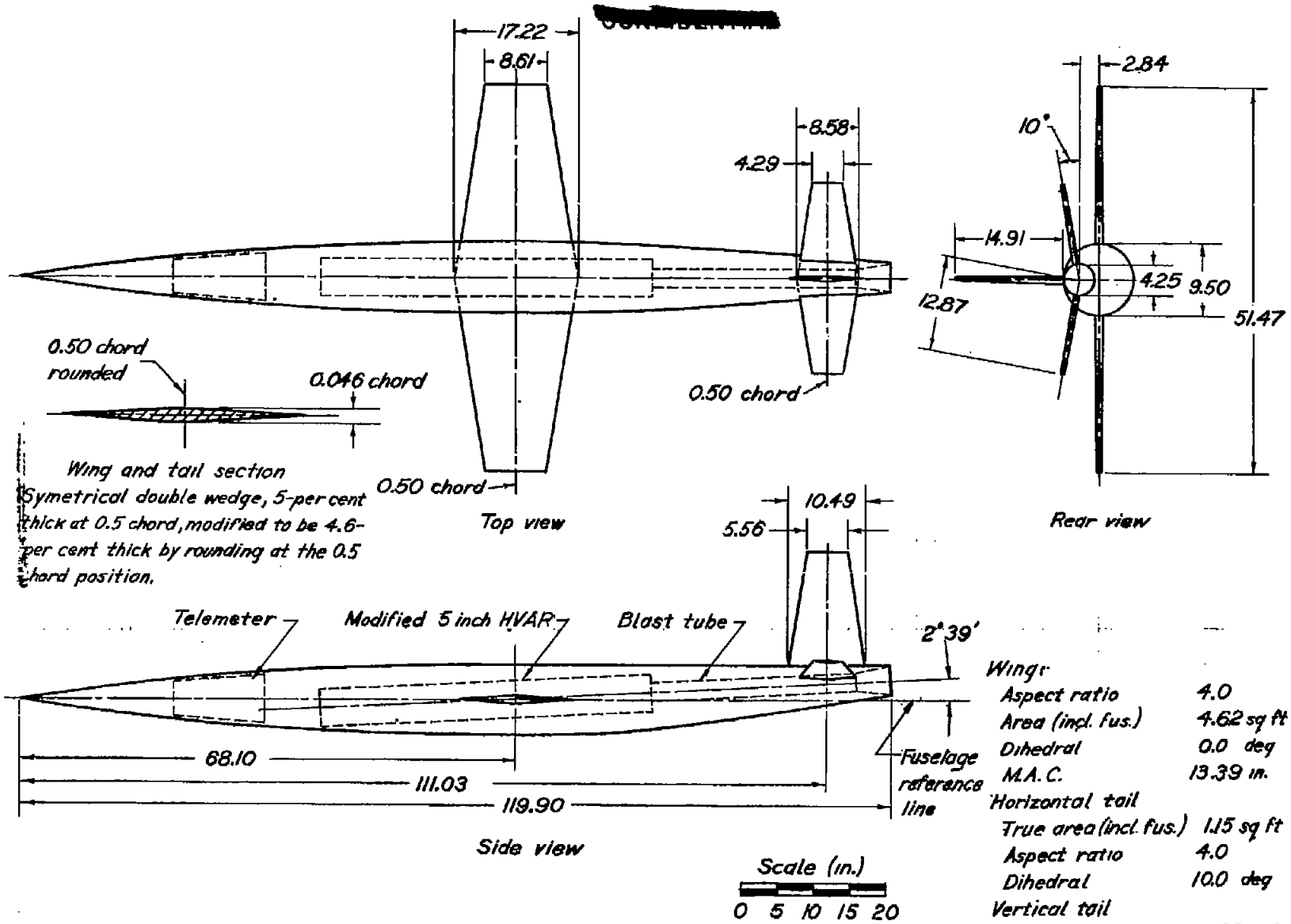

Wing:

Aspect ratio	4.0
Area (incl. fus.)	4.62 sq ft
Dihedral	0.0 deg
M.A.C.	13.39 in.

Horizontal tail

True area (incl. fus.)	1.15 sq ft
Aspect ratio	4.0
Dihedral	10.0 deg

Vertical tail

Exposed area	0.83 sq ft

Figure 1.—General arrangement of the model. All dimensions in inches.

CONFIDENTIAL

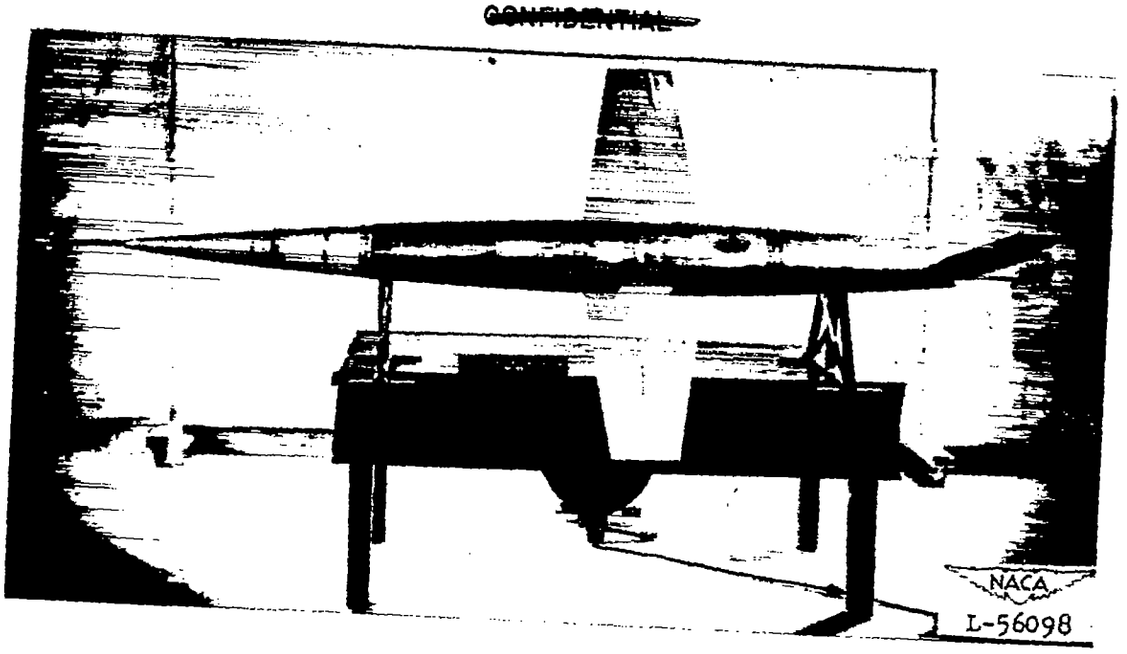

Top view

Side view

Figure 2.- Photographs of the model.

CONFIDENTIAL

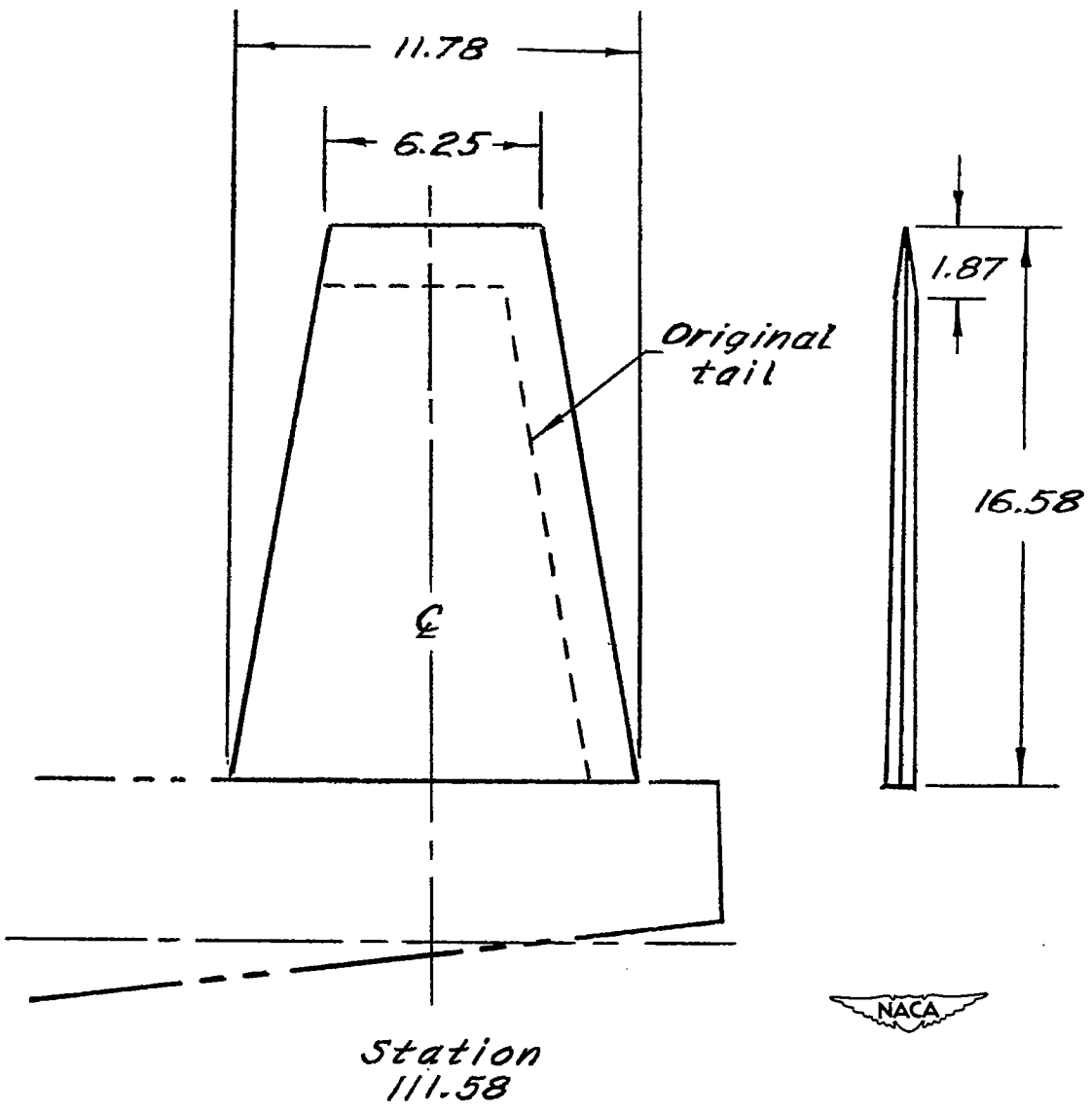

Figure 3.- Sketch of the enlarged vertical tail. All dimensions in inches.

Figure 4.- Photographs of the model on the launcher.

t = 0.6 sec

t = 0.1 sec

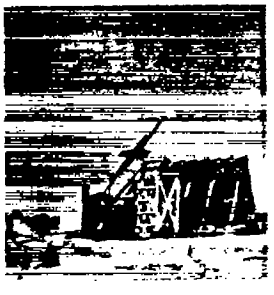

t = -0.4 sec

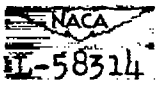

Figure 5.- Photographs of a typical launching.

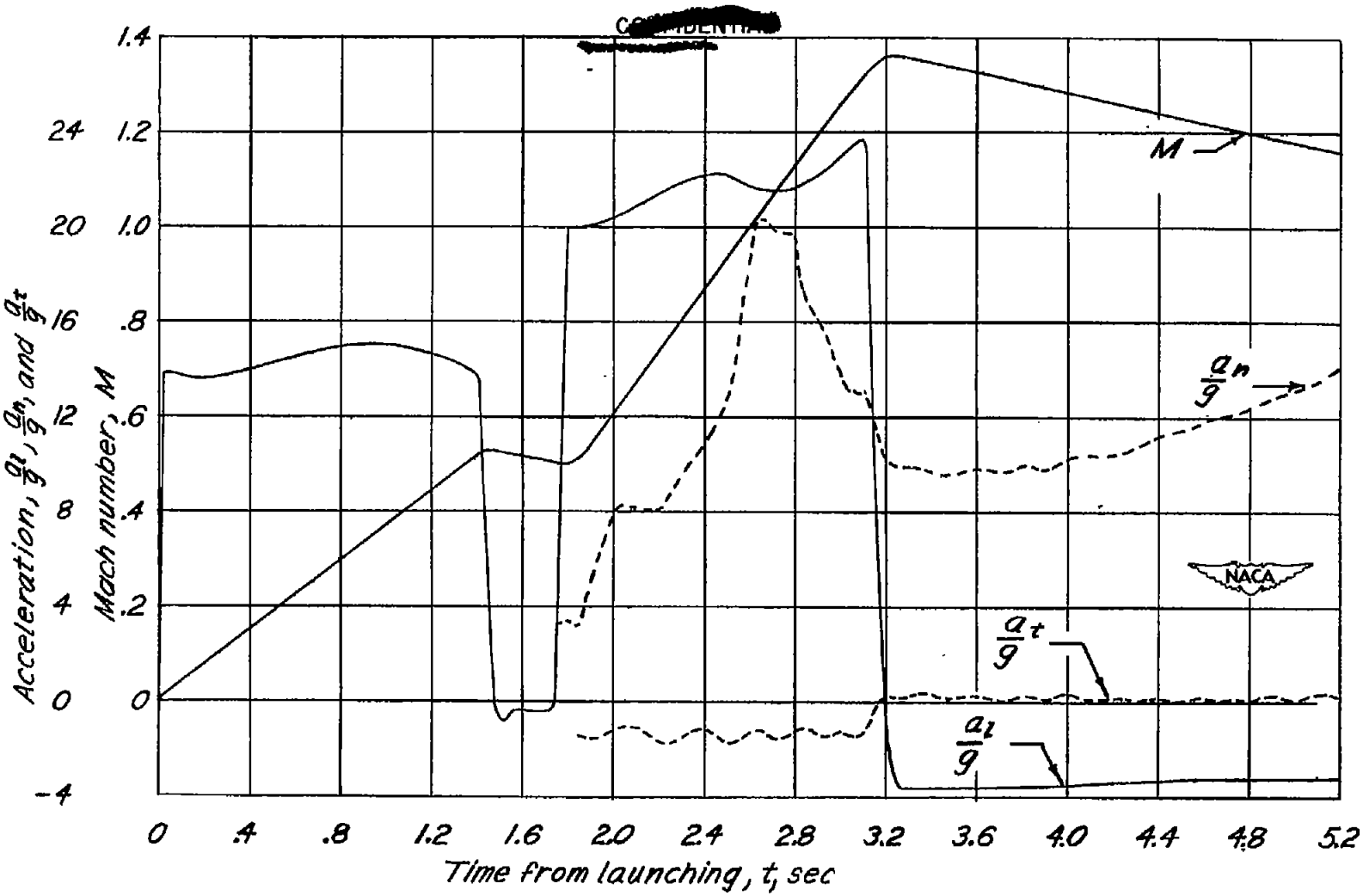

Figure 6. - Time history of the flight of model 1. $\delta = 0°$, center of gravity at $-0.042\bar{c}$.

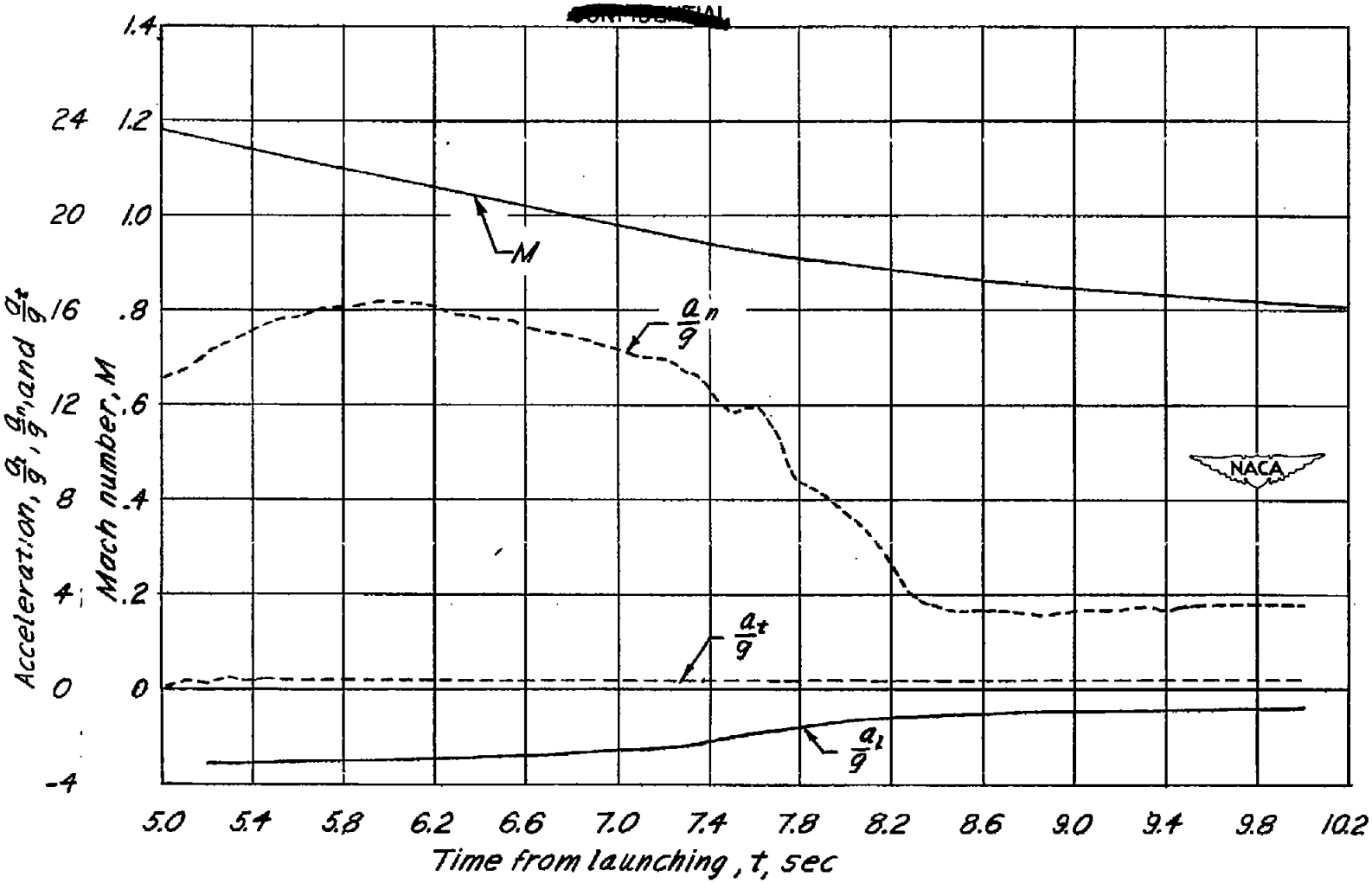

Figure 6.- Concluded.

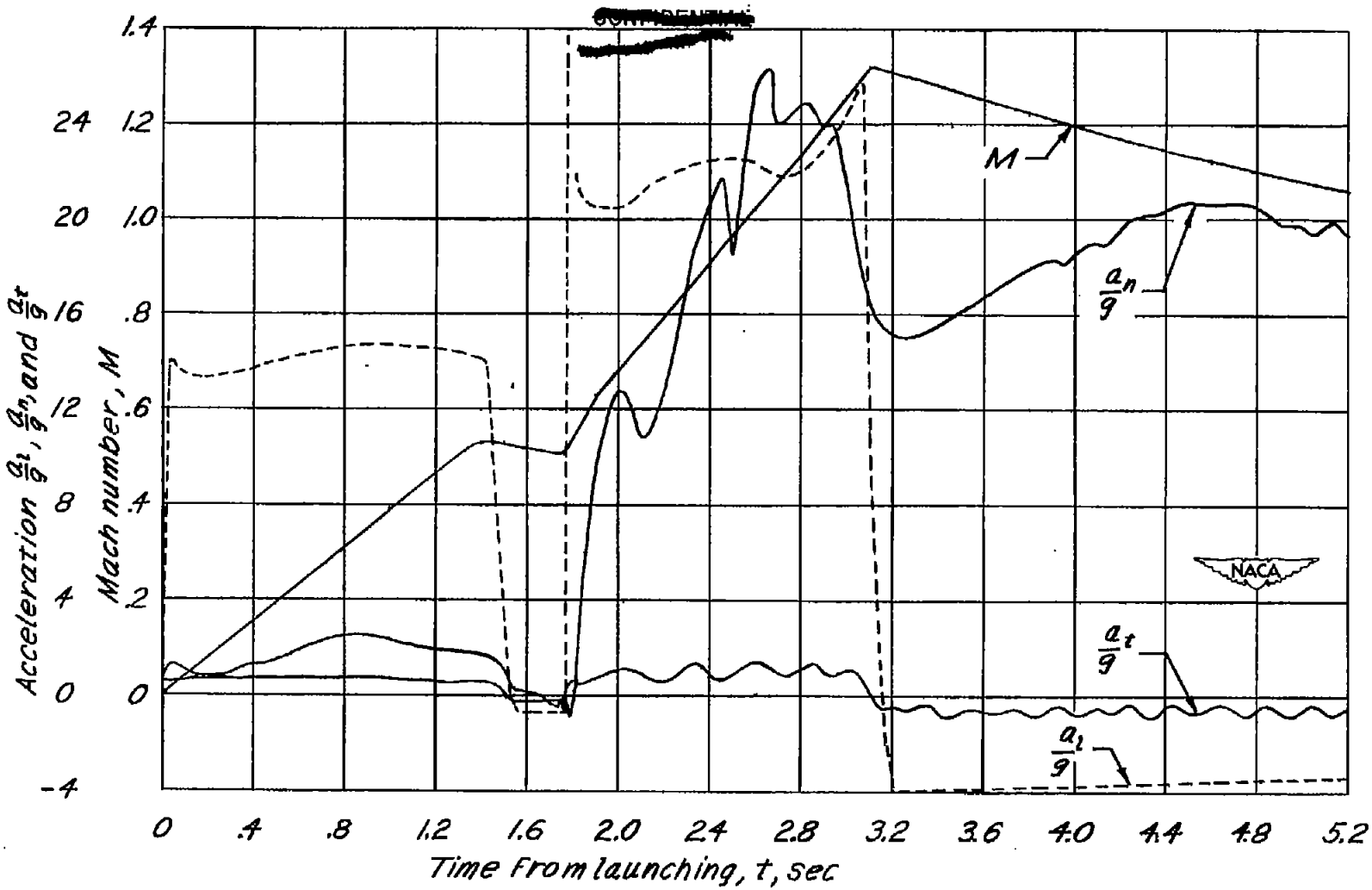

Figure 7.- Time history of the flight of model 2. $\delta = -1.72°$; center of gravity at $-0.047\bar{c}$.

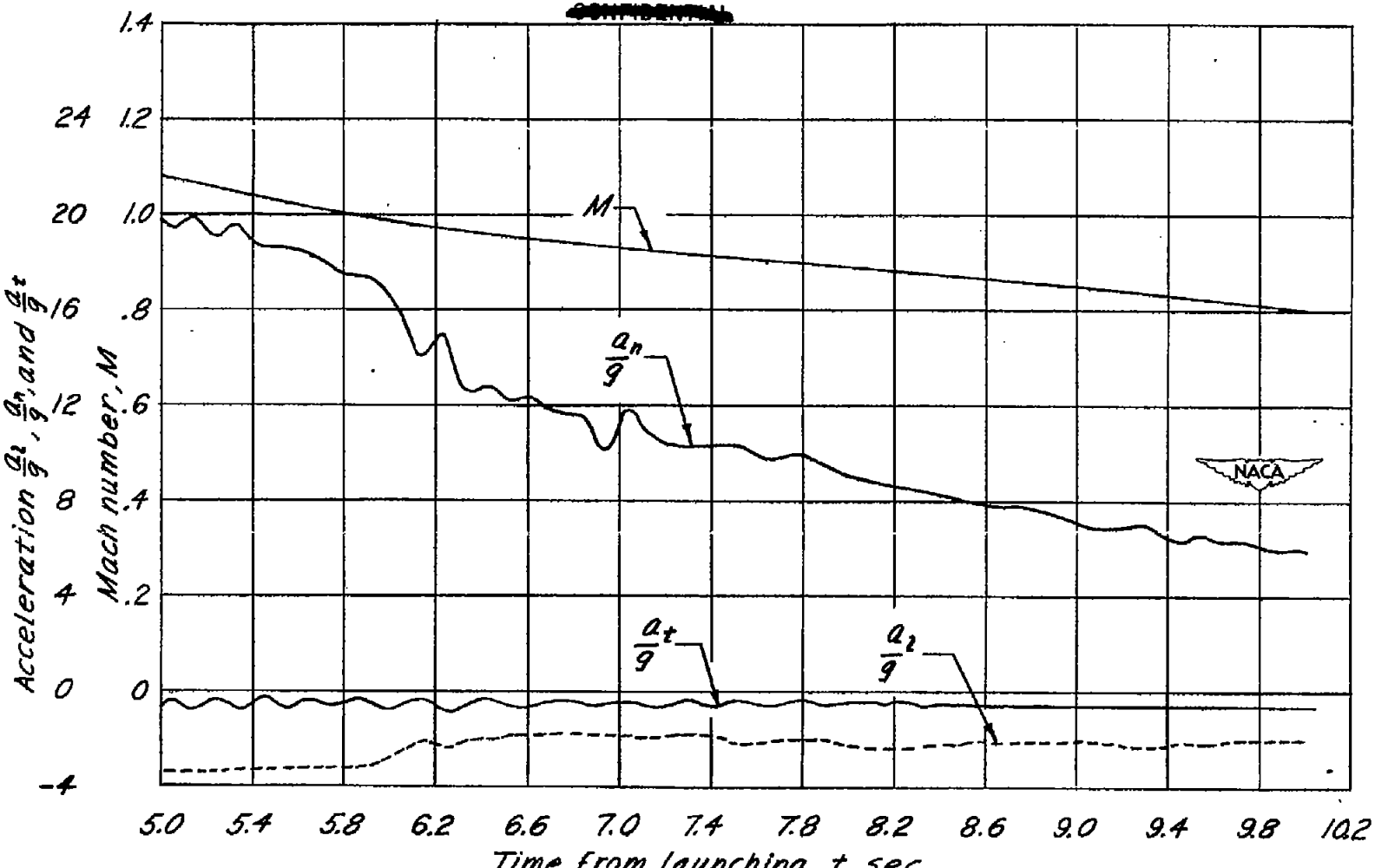

Figure 7.- Concluded.

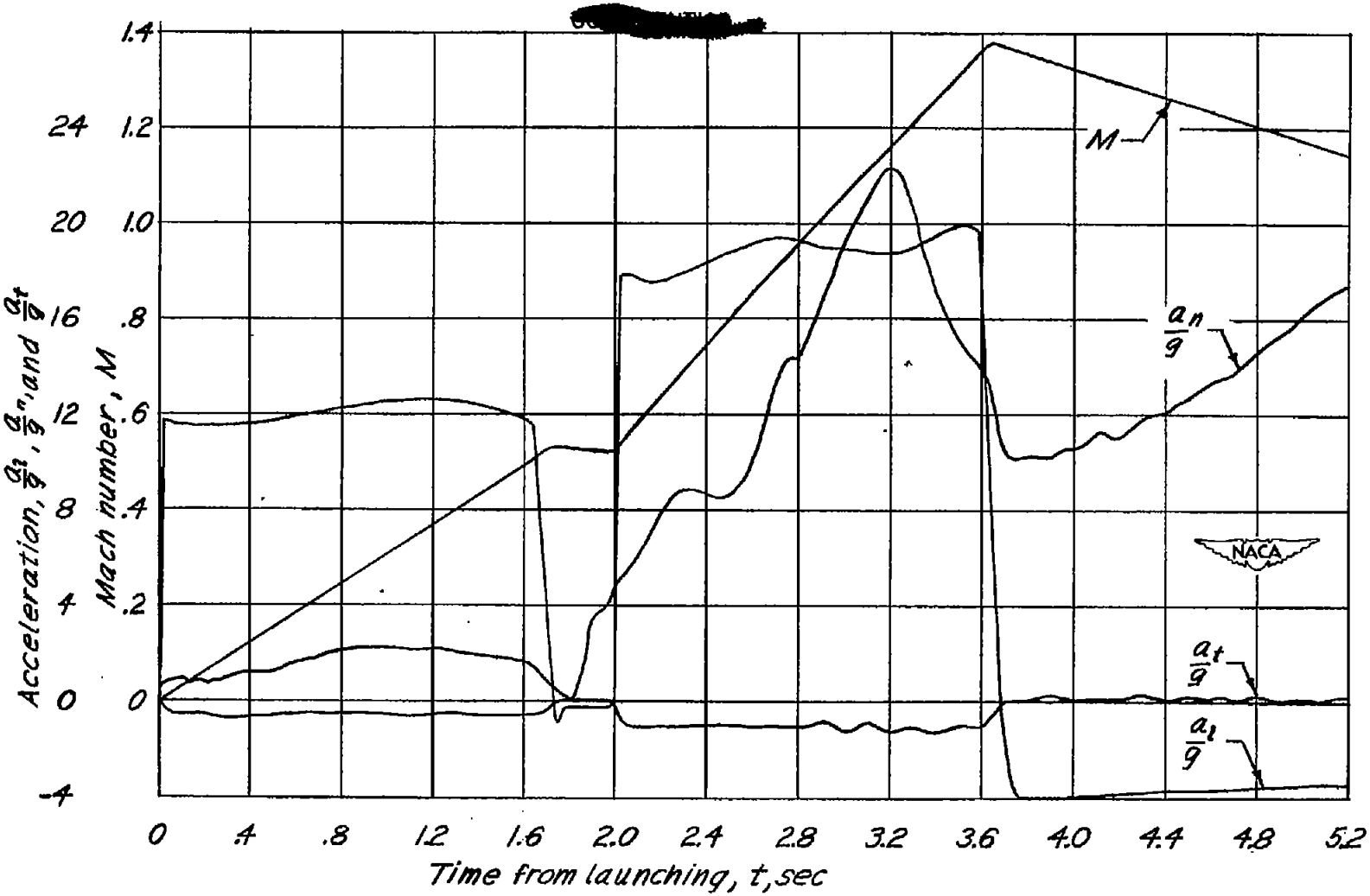

Figure 8 - Time history of the flight of model 3. $\delta = 0.12°$, center of gravity at 0.164 $\bar{c}$

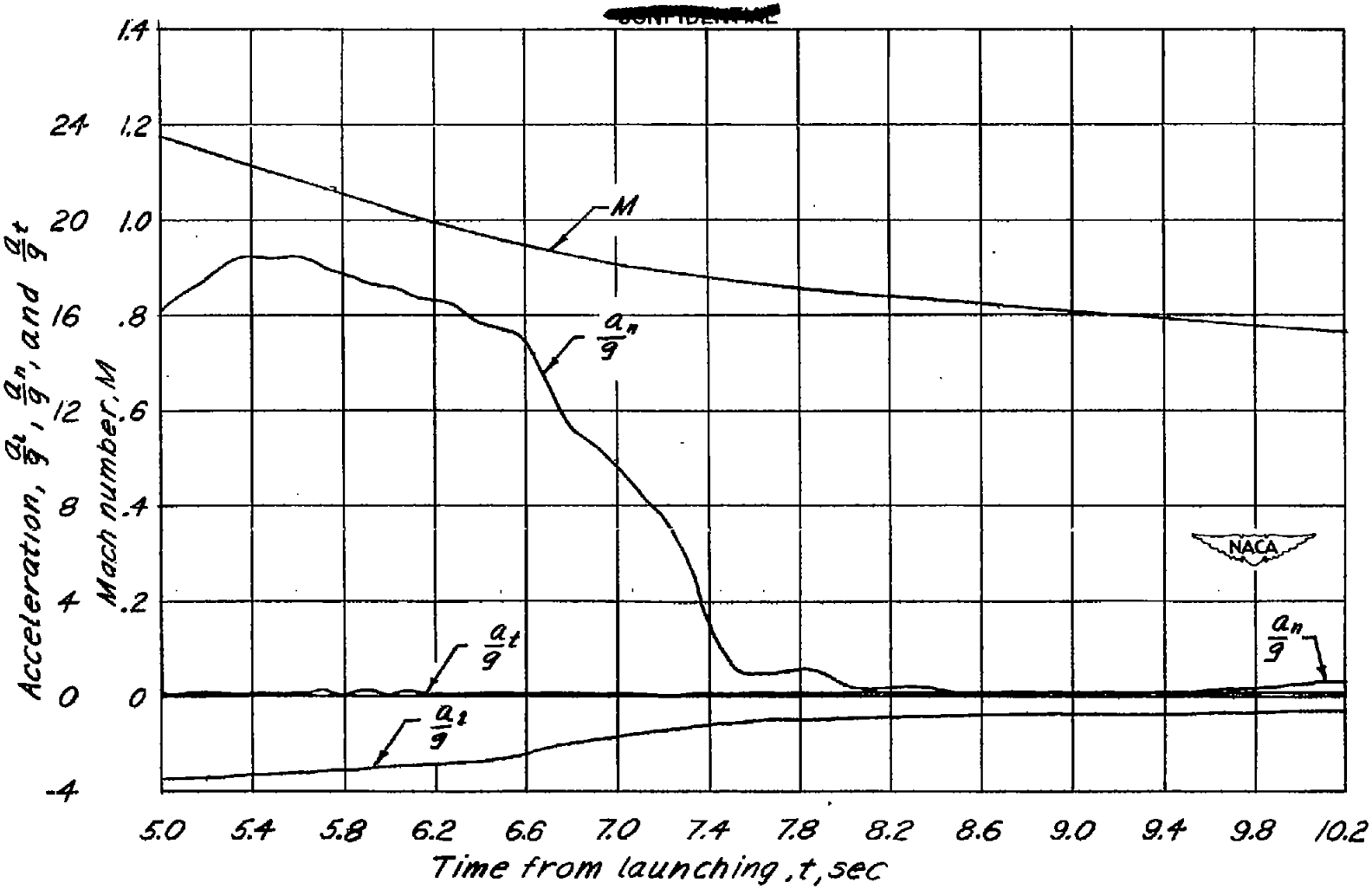

Figure 8.- Continued.

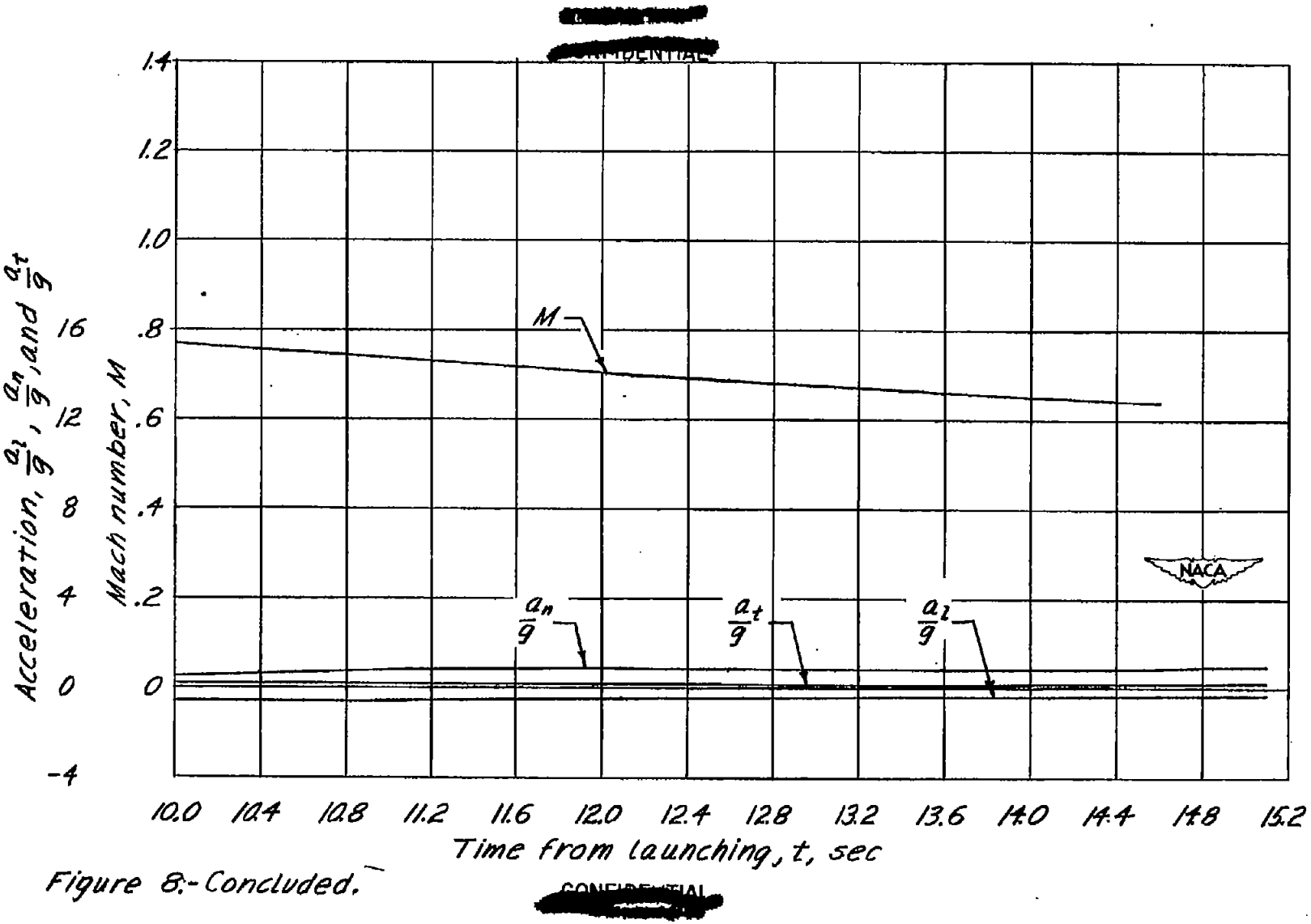

Figure 8.- Concluded.

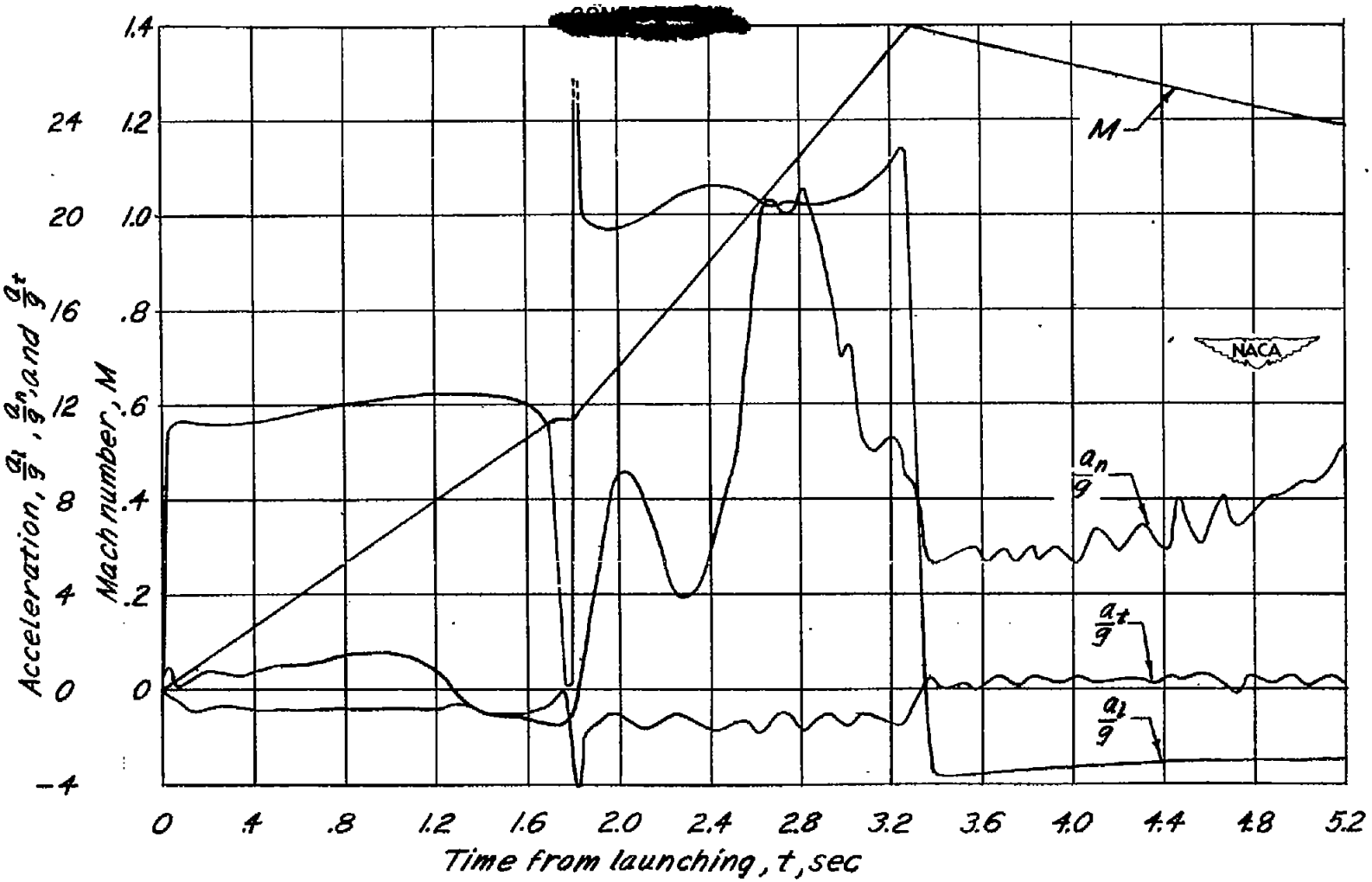

Figure 9.- Time history of the flight of model 4. $\delta = 1.0°$, center of gravity at 0.166 $\bar{c}$.

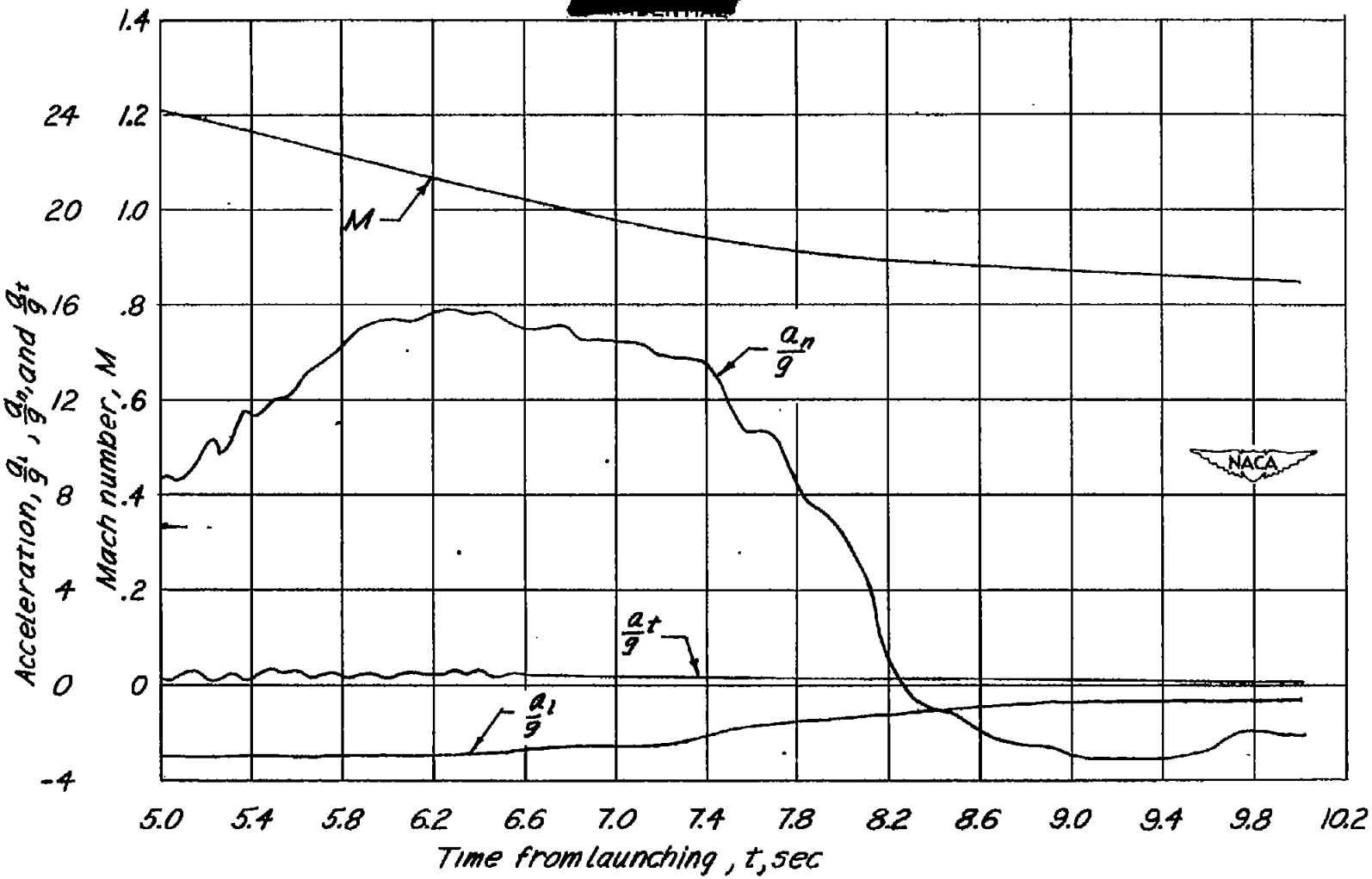

Figure 9.- Concluded.

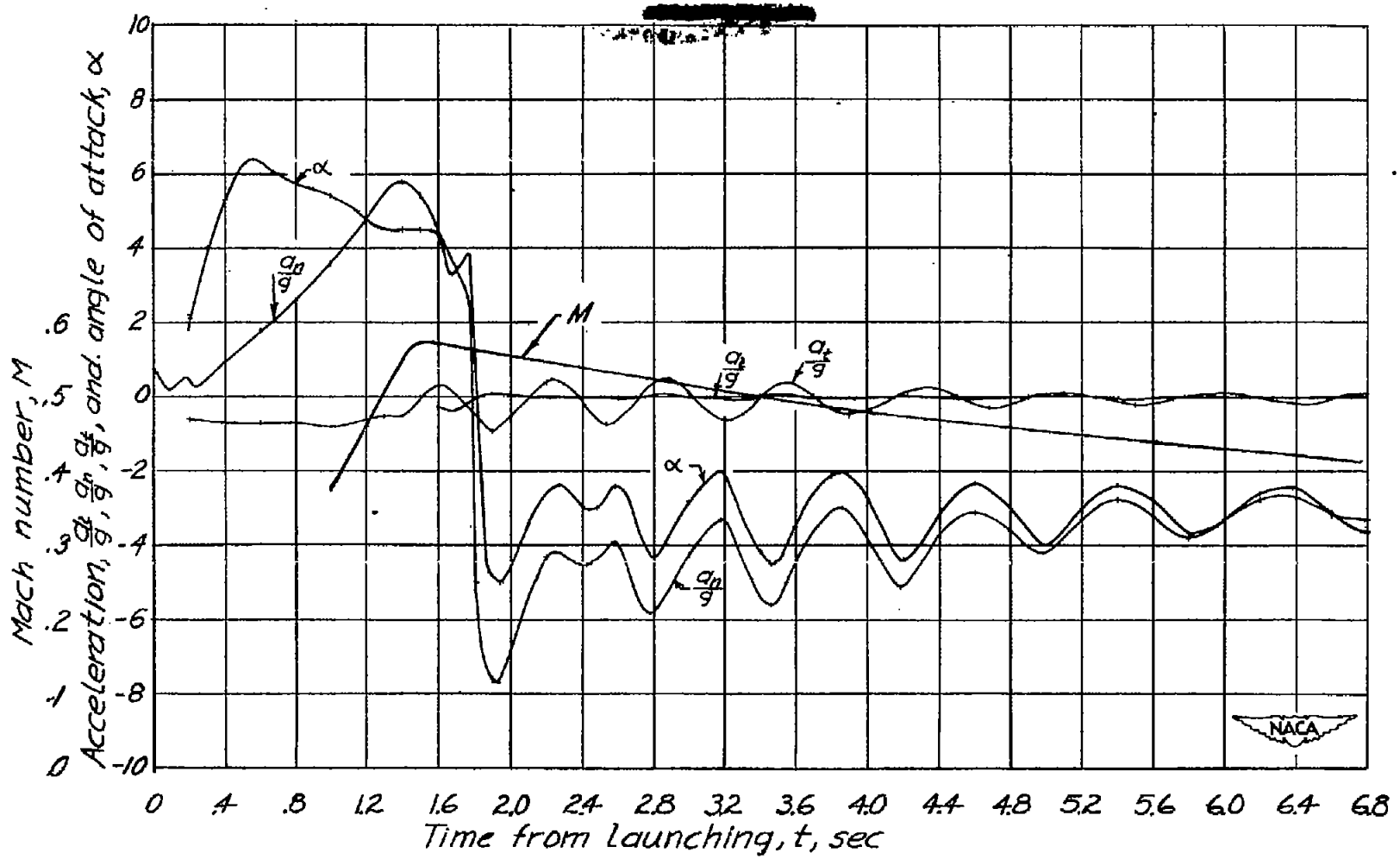

Figure 10.- Time history of the flight of model 5. $\delta = 2.4°$, center of gravity at 0.157 $\bar{c}$.

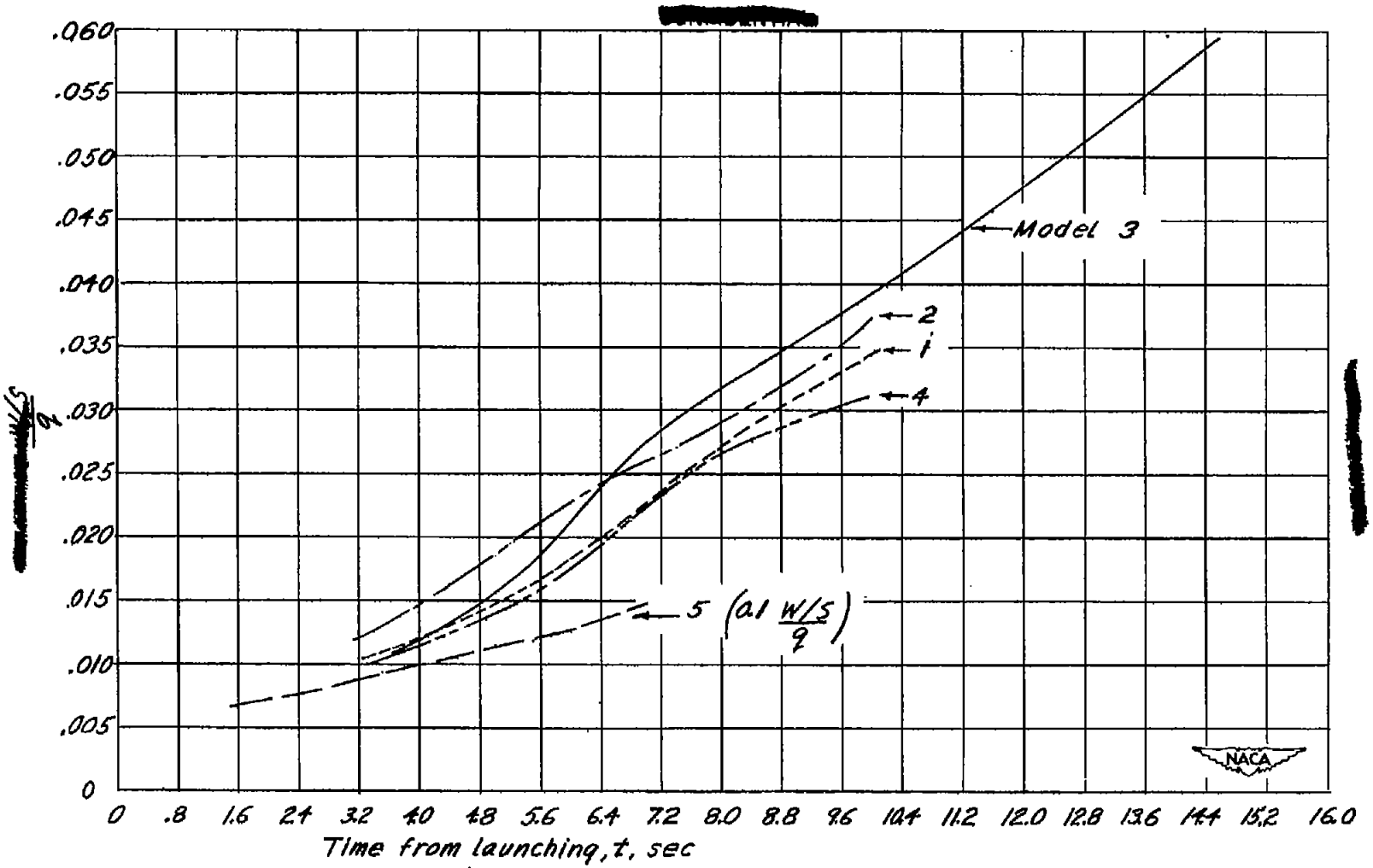

Figure 11.- Variation of $\frac{W/S}{q}$ with time

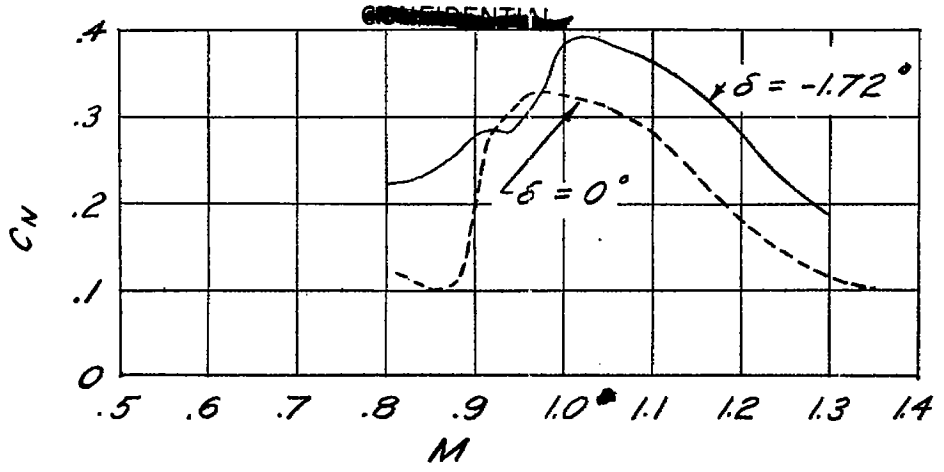

(a) Average center of gravity at -0.045$\bar{c}$.

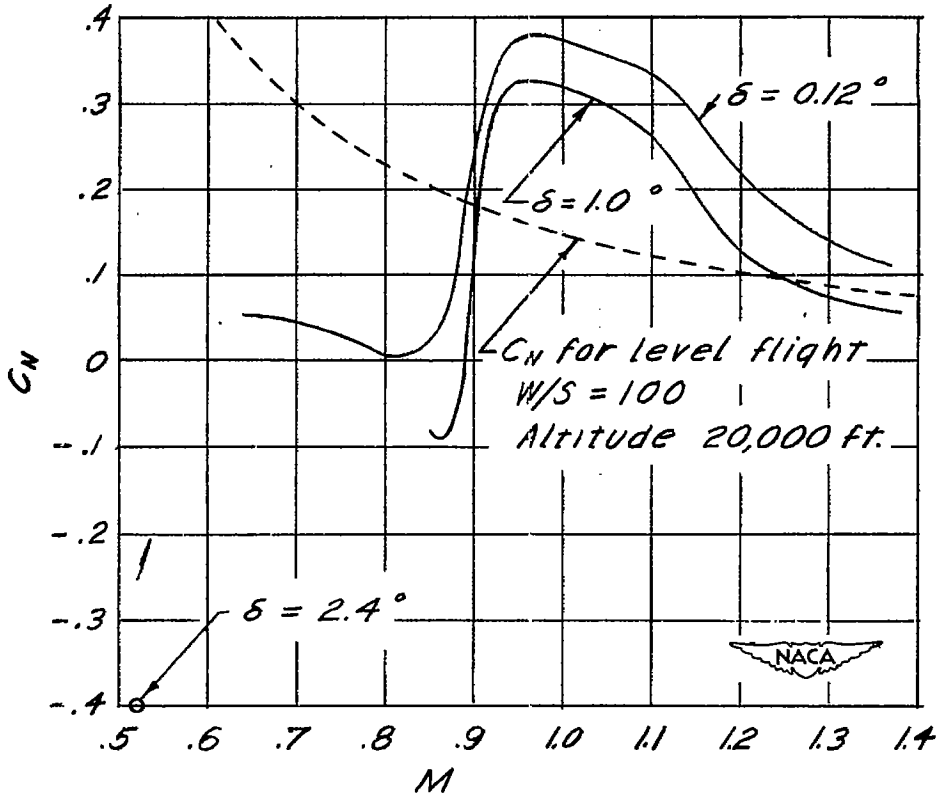

(b) Average center of gravity at 0.16 $\bar{c}$.

Figure 12.- Variation of trim normal-force coefficient with Mach number.

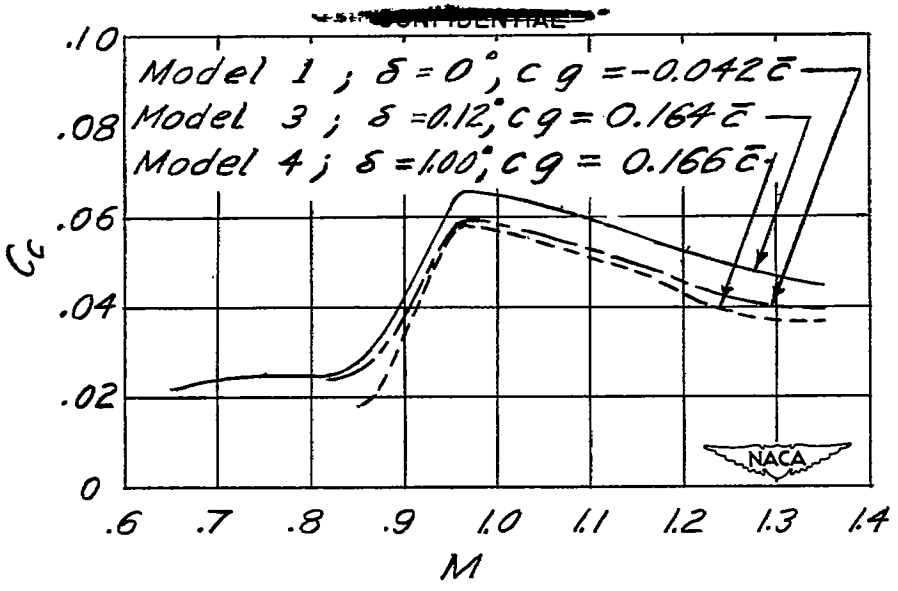

Figure 13.- Variation of chord-force coefficients with Mach number.

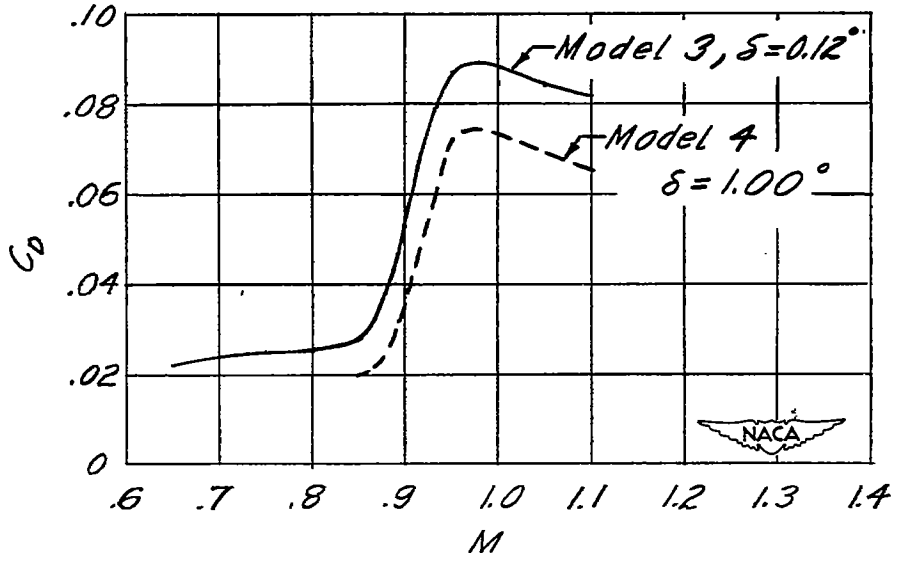

Figure 14.- Variation of trim drag coefficients with Mach number. Center of gravity at 0.16 c̄.

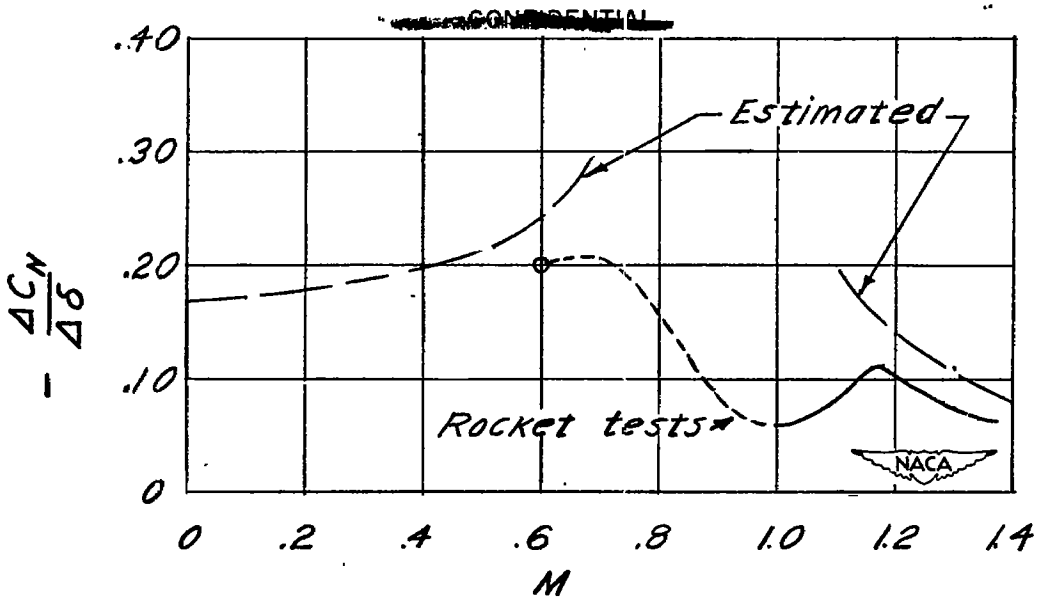

Figure 15.- Variation of control effectiveness with Mach number. Center of gravity at 0.16 $\bar{c}$.

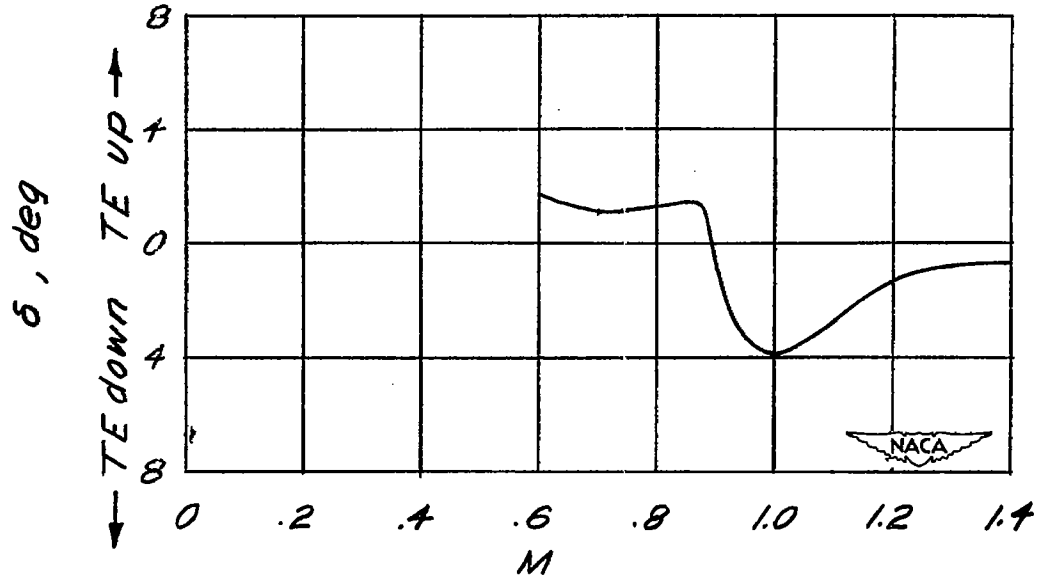

Figure 16.- Horizontal-tail deflection required for trim in level flight. Center of gravity at 0.16 $\bar{c}$, W/S = 100, altitude = 20,000 feet.

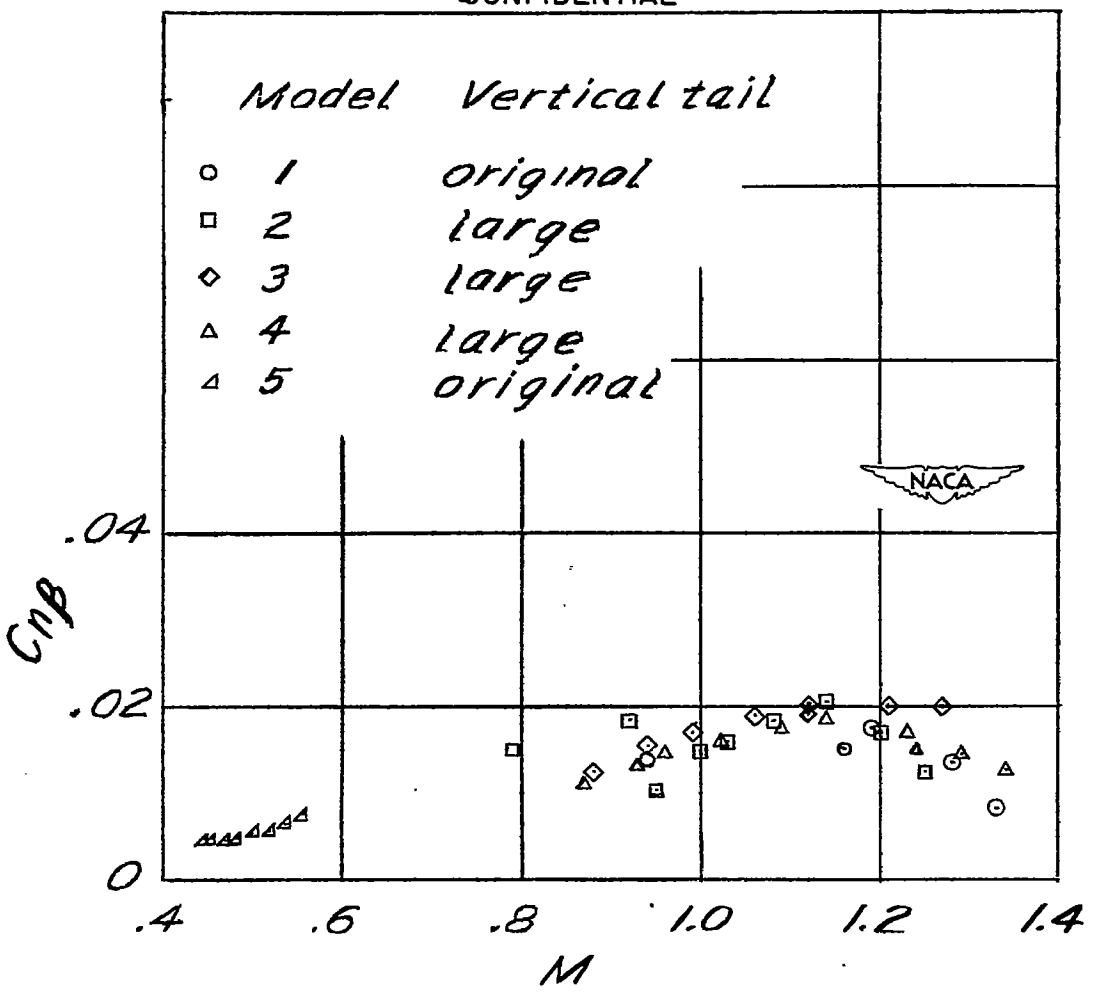

Figure 17.- Variation of the directional stability derivative with Mach number.